JOURNAL OF
Materials
CHEMISTRY

Microstructural aspects of the self-propagating high temperature synthesis of hexagonal barium ferrites in an external magnetic field

Louise Affleck,[a,b] **Marco D. Aguas,**[a] **Ivan P. Parkin,***[a] **Quentin A. Pankhurst**[b] **and Maxim V. Kuznetsov**[b]

[a]*Department of Chemistry, Christopher Ingold Laboratory, University College London, 20 Gordon Street, London, UK WC1H OAJ*
[b]*Department of Physics and Astronomy, University College London, Gower Street, London, UK WC1E 6BT*

Received 28th March 2000, Accepted 5th June 2000
Published on the Web 17th July 2000

Thermal initiation of a mix of BaO_2, Fe_2O_3 and iron powder under a flow of oxygen inside a quartz tube induces a self-propagating reaction with velocity 2 mm s^{-1} and a temperature of *ca.* 975 °C. This leads to the formation of a fused multi-phasic product which on sintering at 1210 °C for 6 h produces phase pure $BaFe_{12}O_{19}$. Reactions were also studied in an applied field of 1.1 T. In this case the pre-ground starting mixture, was attracted to the center of the field and adopted an hour-glass configuration in cross section; initiation of this aligned green mixture under a flow of oxygen produced a propagation velocity of *ca.* 5 mm s^{-1} and a temperature of *ca.* 1150 °C. The product contained two phases, a fused shiny metallic-looking component predominantly from the center of the magnet and a matt red-black coloured component from the edges of the sample. The shiny and matt components were manually separated and analysed both before and after annealing at 1150 °C for 6 h. The effect of changes in reactant particle size of the iron powder, flow of oxygen and addition of an internal oxidising agent ($NaClO_4$) were investigated. Reactions were also studied in which the green mixture was aligned by using two small NdFeB magnets, with the magnets being withdrawn prior to initiation. All the samples both before and after annealing were characterised by X-ray powder diffraction, infrared, vibrating sample magnetometry, scanning electron microscopy, energy dispersive analysis by X-rays, electron microprobe analysis and Mössbauer spectroscopy. The sintered ferrites showed comparable remanence (σ_r) and maximum magnetisation σ_{max} to conventionally prepared samples, but significantly lower coercivity.

Self-propagating high temperature synthesis (SHS) is a fast, solid-state method for making a range of ceramic, metallic and intermetallic materials.[1] The reactions proceed by an exothermic chemical reaction that is violent enough to ignite successive layers of reactant and progress by means of a synthesis wave (also known as a thermal flash or propagation wave).[2] SHS reactions typically involve elemental combinations or reactions between elements and metal oxides [eqn. (1)].[3–5]

$$M + yE \rightarrow ME_y \qquad (1)$$

(M = metal, E = non metal)

R. B. Kaner *et al.*[6] and ourselves[7] have developed a sub-branch of SHS reactions known as solid-state metathesis reactions (SSM). These reactions occur between anhydrous metal halides and alkali or alkali earth metal pnictides, chalcogenides, carbides or borides. The reactions are as exothermic as the traditional SHS reactions. The driving force in SSM reactions is the formation of a co-produced salt. This salt limits the maximum reaction temperature (to the boiling point of the salt) and also acts as a wetting agent that allows the diffusion of reactants.[8] In these syntheses and other SHS reactions it is normal for the reaction to involve two stages; the initial SHS reaction followed by a relatively short period of annealing. If the SHS reaction is conducted on a sufficiently large scale (*ca.* kg) then the second annealing stage to produce a single phase of material is often not required. The reaction has sufficient thermal mass that the cool down rate is slow enough to allow complete reaction. On smaller scale reactions the initial SHS process can produce a variety of partially formed products, intermediates and unreacted starting materials.[9,10] This initially formed SHS mass is readily annealed to form the final product as the reactive components are highly mixed and solid-state diffusion-distances are minimised.[11] In general the composition and microstructure of the as-formed SHS materials have not been studied in detail.

We have a particular interest in the formation of magnetic oxide materials by SHS reactions, especially those incorporating iron metal.[12] These systems have enabled interrogation of compositional, morphological and magnetic microstructure by a variety of techniques including magnetometry, diffraction and ^{57}Fe Mössbauer techniques.[12] We have reported the first studies of the effects of an external magnetic field on an SHS reaction for a representative series of hard hexagonal ferrites[13] and soft ferrites[14,15] such as $Li_{0.5}Fe_{2.5}O_4$, $MgFe_2O_4$ and $ZnFe_2O_4$. The reactions were performed in a two-stage manner, an initial SHS reaction followed by grinding and annealing for 4–6 h. It was noticeable that the magnetic properties of the materials synthesised in an external field during SHS were often very different to those formed in the absence of a field.[13,14] By adjustment of the reaction variables it was possible to show that the external field had a pivotal role in the course of the reaction and in the properties of the products, even after prolonged post SHS annealing above the Curie temperature. Examples of changes in magnetic properties of the sintered material included a 100% reduction in coercivity between applied field (AF) and zero field (ZF) $BaFe_{10}Cr_2O_{19}$[13] and a 30% change in remanent magnetisation for $MgFe_2O_4$.[15]

It was also observed that the applied field SHS proceeds with a greater reaction temperature and with faster propagation velocity.[16,17] One tentative explanation for these effects relies on prior organisation of the green mixture particularly of the magnetic iron fuel source along magnetic field lines. This prior organisation allows for an easy propagation direction for the

DOI: 10.1039/b002431g

reaction front, a more complete reaction, and hence elevated temperatures compared to the zero field reactions.

Previously we have shown that initiation of a pre-ground mixture of barium peroxide, iron and iron oxide induces an exothermic chemical reaction that proceeds from the point of initiation with uniform velocity.[12] The reaction produced a partly fused mass, which on annealing at 1150 °C for 6 h, produces phase pure $BaFe_{12}O_{19}$. In our previous work we typically studied the reaction on a relatively large scale and in air and were somewhat selective in choosing only the fused part of the product for further investigation.[13] In the fused segment the appearance of the barium ferrite phase was observed directly from the SHS reaction. It should be noted that the as-formed SHS product was not phase pure and often contained unreacted starting material in addition to some partly reacted material. In order to try and explain the differences in magnetisation between the zero field and applied field reactions we decided to investigate in detail the products formed after the initial SHS reaction.

In this paper we report a study into the microstructures formed by SHS reactions of barium peroxide, iron and iron oxide in zero and an applied magnetic field. In particular we investigate the changes in synthesis temperature and propagation wave velocity with reaction conditions, particle size and magnetic field. The materials as-formed in the SHS reaction have been examined in detail to determine the completeness of the reaction. We further report two distinct regions of product formed in the applied field synthesis, a shiny, fused component and a matt, friable component.

Experimental

All reagents were obtained from Aldrich Chemical Co. and used as supplied. A commercial sample of $BaFe_{12}O_{19}$ was obtained from Sakai Chemical Industries, Osaka. All reagents were checked for phase and elemental purity by X-ray powder diffraction (XRD) and energy dispersive X-ray analysis (EDAX) prior to use. The general experimental techniques and apparatus used have been described before[13] with the following additions. X-Ray diffraction patterns were also obtained on station 9.1 at the CLRC Daresbury Laboratory using an image plate system, samples were loaded for this measurement in quartz capillary tubes. Pre-alignment X-ray diffraction studies in a magnetic field were also studied at the Daresbury Laboratory on Station 16.4 using the energy dispersive mode. Electron microprobe experiments were conducted on a JEOL EMA. Propagation velocities were determined *via* stopwatch. Synthesis wave temperatures were determined by optical pyrometry and by a FLIR thermal imaging camera.

Preparation of $BaFe_{12}O_{19}$ in zero field

BaO_2 (1.196 g, 10 mmol), iron powder (2.573 g, 48 mmol) and Fe_2O_3 (3.84 g, 24 mmol) were ground together in a pestle and mortar. The resulting powder was placed inside a quartz tube under a flow of oxygen of 2 l min^{-1}. The mixture was initiated by means of a nichrome filament at 800 °C. This produced an orange propagation wave (975 °C) that travelled through the material at *ca.* 2 mm s^{-1}. The powder darkened to brown after the propagation wave had passed and became partly fused. The brown material, both as-prepared and after annealing at 1150 °C for 6 h, was analysed by X-ray powder diffraction, Table 1, electron probe analysis and scanning electron microscopy/energy dispersive analysis by X-rays, Table 2, vibrating sample magnetometry, Table 3 and Mössbauer spectroscopy, Table 4. The infrared spectra of the sintered hexagonal barium ferrite showed a broad band at 600 cm^{-1}.

Reactions in a magnetic field

The same scale and procedure was used as in the zero field reactions except the quartz tube was placed inside a 1.1 T Halbach cylinder magnet. The whole of the pre-ground powder was attracted into the center of the magnetic field and adopted an hour-glass configuration in cross section, Fig. 1a. An oxygen flow of *ca.* 2 l min^{-1} was started and the reaction initiated by means of a hot nichrome filament. This produced an orange–yellow propagation wave that travelled at 5 mm s^{-1} and temperature 1210 °C. Some structuring of the product was noted after the reaction with two horizontal hollow grooves at the edges of the powder. The product had a metallic-grey shiny component, originating from the center of the magnetic field, and a matt red–brown appearance for the material at the edges of the magnet. Both components were removed from the field by forcing a plunger along the length of the tube. The two components were manually separated. Both shiny and matt components were ground and sintered at 1150 °C for 6 h and analysed as outlined above for the zero field reactions.

Reaction of a pre-magnetised green mixture

The same scale and procedure was used as in the zero field reactions. The green mixture was placed into a quartz tube and magnetised by bringing up two (2 cm diameter) neodymium iron boron permanent magnets (*ca.* 0.2 T, Fig. 1b). The magnets caused the green mixture to become orientated, adopting a partial hour-glass configuration in cross section. The magnets were removed at right angles from the hour-glass axis. Despite removal of the magnets the green mixture kept the same orientation. Oxygen gas was allowed to flow along the tube (2 l min^{-1}) and an SHS reaction initiated by means of a heated nichrome filament. The propagation velocity was 2 mm s^{-1} and the propagation temperature was 1150 °C. The product consisted of shiny silver globules and a matt brown powder. These components were manually separated and both analysed as above.

Variation in reaction conditions

The same reaction scale and procedure was adopted as described in the zero field experiments except for the following modifications. Three different grades of iron powder of average particle size 10 μm, 44 μm and 500 μm were used (*ca.* 90% of the particles were within 25% of the mean particle size). Various amounts of an internal oxidising agent such as sodium perchlorate were added to the green mixture. The grinding stages using sodium perchlorate were accomplished by grinding together all of the reaction components with the exception of the sodium perchlorate. This was added to the green mixture that was then lightly ground. The products from the perchlorate reactions were washed with water (2 × 250 ml) prior to sintering. In all reactions involving sodium perchlorate the product was black and fused. In the applied field and zero field perchlorate reactions a trace shiny globular component was seen. The propagation velocities and reaction temperatures are listed in Table 2.

Caution: SHS reactions can be very exothermic, sometimes explosively, so with any new system care should be taken to carry out the reactions behind a blast proof screen. High temperature material can be ejected from the site of a laboratory scale reaction up to 1 m. Sodium perchlorate is a very strong oxidising agent, combination with some metal powders can cause an explosive oxidation to occur. Although we have used sodium perchlorate in these reactions over two hundred times and had no adverse reaction and in no case did the green mixture ignite on grinding, it is anticipated that grinding sodium perchlorate and iron powder could be particularly hazardous. In all reactions the overall scale was

Table 1 X-Ray powder diffraction data for the SHS reactions of iron, iron oxide, barium peroxide and sodium perchlorate in zero field (ZF), an applied field of 1.1 T (AF) and a prealigned field of 0.2 T. Phases identified prior to sintering are listed in order of abundance as determined by scanning electron microscopy and correlated by X-ray powder diffraction measurements. Literature lattice parameters for $BaFe_{12}O_{19}$ were $a = 5.889(1)$, $c = 23.190(7)$ Å,[12] lattice parameters for the commercial $BaFe_{12}O_{19}$ were $a = 5.897(2)$, $c = 23.212(3)$ Å.

Reaction conditions	Phases identified prior to sintering	Phase identified after sintering	Lattice parameters observed/Å
$BaO_2 + Fe + Fe_2O_3$ ZF[a]	Fe_2O_3, Fe, $BaFe_2O_4$, Fe_3O_4, FeO	$BaFe_{12}O_{19}$[d]	$a = 5.889(2)$ $c = 23.216(7)$
$BaO_2 + Fe + Fe_2O_3$ AF[b]—matt	Fe_2O_3,$BaFe_2O_4$, Fe, FeO, Fe_3O_4,	$BaFe_{12}O_{19}$	$a = 5.889(3)$ $c = 23.210(10)$
$BaO_2 + Fe + Fe_2O_3$ AF—shiny	Fe_3O_4, $BaFe_2O_4$, FeO, Fe_2O_3	$BaFe_{12}O_{19}$	$a = 5.895(3)$ $c = 23.229(10)$
$BaO_2 + Fe + Fe_2O_3$ pre-aligned[c]—matt	Fe, Fe_2O_3, Fe_3O_4, $BaFe_2O_4$, FeO	$BaFe_{12}O_{19}$	$a = 5.890(3)$ $c = 23.219(10)$
$BaO_2 + Fe + Fe_2O_3$ pre-aligned—shiny	Fe_3O_4, $BaFe_2O_4$, FeO, Fe_2O_3, Fe	$BaFe_{12}O_{19}$	$a = 5.894(2)$ $c = 23.241(7)$
$BaO_2 + Fe + Fe_2O_3 + NaClO_4$ ZF	Fe_3O_4, FeO, $BaFe_2O_4$	$BaFe_{12}O_{19}$[d]	$a = 5.885(2)$ $c = 23.235(12)$
$BaO_2 + Fe + Fe_2O_3 + NaClO_4$ AF	Fe_3O_4, FeO, $BaFe_2O_4$	$BaFe_{12}O_{19}$	$a = 5.888(3)$ $c = 23.260(12)$
$BaO_2 + Fe + Fe_2O_3 + NaClO_4$ pre-aligned	Fe_3O_4, FeO, $BaFe_2O_4$	$BaFe_{12}O_{19}$[d]	$a = 5.891(2)$ $c = 23.235(7)$

[a] ZF = synthesis carried out with zero field. [b] AF = synthesis carried out under an applied filed of 1.1 T. [c] Pre-aligned = synthesis carried out by aligning the green mixture with a 0.2 T field, the field is withdrawn prior to synthesis. [d] A minor *ca.* 2% component of $BaFe_2O_4$ was also detected.

kept to *ca.* 1 g for trial reactions before scaling up to 10 g of material. Barium peroxide is very toxic.

Results

Synthesis and characterisation

The overall reaction between barium peroxide, iron and iron oxide can be idealised by eqn. (2). In actuality, the molar ratios of the starting reagents used in the synthesis were $BaO_2 : Fe : Fe_2O_3$; 1 : 4.8 : 2.4. That is, an excess of barium peroxide is used in the reaction. This was found to be necessary in this system to ensure that single phase $BaFe_{12}O_{19}$ is formed. Some barium is volatilised during the SHS and sintering processes as barium oxide.

$$BaO_2 + 6Fe + 3Fe_2O_3 + 4O_2 \rightarrow BaFe_{12}O_{19} \qquad (2)$$

The reaction only goes to completion after two stages, an initial SHS reaction followed by a sintering stage at 1150 °C for 6 h. The as-formed SHS product shows a mixture of unreacted starting material, partially reacted material and the formation of significant quantities of intermediates. The extent and nature of the materials formed will be discussed in detail below. At this stage it should be pointed out that in no case was the $BaFe_{12}O_{19}$ phase unambiguously identified in the 'as-formed' SHS product. However the initial SHS stage produces in all cases a solid that is exceptionally reactive with good contact between neighbouring grains that enables a rapid transformation to the hexagonal ferrite on annealing. This transformation is faster than the conventional synthesis of hexagonal ferrites (6 h compared to 24 h) and involves far fewer steps (the conventional route has twelve separate operations),[12] and as discussed below, the ferrites produced by the SHS route have somewhat unusual magnetic properties.

The extent of the SHS reaction is determined by the particle size of the reagents, use of an external magnetic field, the oxygen flow and the addition of an internal solid oxidising agent. The whole SHS process is driven by the oxidation of iron metal from Fe(0) to Fe(III) in $BaFe_{12}O_{19}$; a reaction with an exothermicity of *ca.* 900 kJ mol^{-1}.[12] The iron(III) oxide added to the starting mixture acts as a moderator and also becomes incorporated in the product. This reagent is important because in its absence on a laboratory scale of 10 g, the SHS reaction can eject material at *ca.* 1000 °C up to 1 m from the reaction site. The limiting reagent in the reaction is oxygen. Oxygen is incorporated into the products in three ways, firstly the decomposition of barium peroxide provides an internal intimately mixed source of oxygen, secondly oxygen gas is pumped into the reaction and thirdly in some reactions sodium perchlorate was added to the reaction mix. The sodium perchlorate provided an additional source of oxygen, produced sodium chloride—that acted as a wetting agent—and on decomposition released additional energy for the reaction.

Zero field reactions

Analysis of the product formed from the reaction of barium peroxide, iron and iron(III) oxide under an oxygen atmosphere in the absence of an external magnetic field indicates that the product is polyphasic. Inspection by optical microscopy reveals on a macroscopic scale that the product is relatively homogeneous, of a single colour and has no external structuring. On a microscopic scale however, a combination of Mössbauer (Fig. 2 and 3), EDXA and X-ray powder diffraction (Fig. 4) analysis show that the product consists of five phases. In order of abundance these were Fe_2O_3, Fe, $BaFe_2O_4$, Fe_3O_4 and $Fe_{1-x}O$. Thus, even though a propagation wave passes through the whole solid at *ca.* 975 °C, only 40–50% of the reactants are converted. Virtually all of the barium peroxide has been decomposed in the reaction, although some regions (*ca.* 10%) showed completely unreacted pockets of

Table 2 Propagation velocity, temperatures and microstructure of the products from the SHS reactions of iron, iron oxide, barium peroxide and sodium perchlorate in zero field (ZF), an applied field of 1.1 T (AF) and a pre-alignment field of 0.2 T

Description	Physical appearance	Electron microprobe	Propagation temperature/°C	Propagation velocity/mm s^{-1}
BaF, zero field	Matt red–brown powder	Homogeneous	975	2
BaF, applied field, matt	Matt red–brown powder	Homogeneous	1210	5
BaF, applied field, shiny	Shiny silver coloured product, 60–70% fibrous structure alligned along field axis	Acicular particles (100 μm × 10 μm) with a 1 : 12 Ba : Fe ratio, makes up 90% of area	1210	5
BaF, pre-aligned, matt	Matt red–brown powder	Homogeneous	1150	2
BaF, pre-aligned, shiny	Shiny silver coloured, 30–40% globules, partly fibrous structure	Smooth areas 1 : 12 Ba : Fe ratio. No acicular particles	1150	2
BaF perchlorate, zero field	Fused lump, dark grey–black		1250	>2
BaF perchlorate, applied field	Fused black lump, no fibrous structure	Some *ca.* 10% acicular particles with a 1 : 12 Ba : Fe ratio *ca.* 50 × 20 μm	1250	>5
BaF perchlorate, pre-aligned	Fused black lump	Homogeneous	1250	>5

Table 3 Coercivity, saturation magnetisation and remanent magnetisation of the pre- and post-sintered (1150 °C, 6 h) SHS reaction of iron, iron(III) oxide and barium peroxide

	Post SHS			Sintered		
Description	σ_{max} ±0.1 (emu g^{-1})	σ_r ±0.1 (emu g^{-1})	H_c ±0.01 (kOe)	σ_{max} ±0.1 (emu g^{-1})	σ_r ±0.1 (emu g^{-1})	H_c ±0.01 (kOe)
Zero field	21.7	3.6	0.26	49.5	35.2	2.13
Applied field, matt	40.1	9.9	0.19	47.3	32.8	2.02
Applied field, shiny	46.9	10.7	0.16	44.3	29.3	1.60
Pre-aligned, matt	42.9	8.3	0.25	47.6	32.7	2.35
Pre-aligned, shiny	26.3	7.9	0.33	55.6	38.8	1.82
Perchlorate, zero field	48.1	8.8	0.13	46.5	30.4	1.40
Perchlorate, applied field	59.6	13.4	0.13	49.4	31.2	1.23
Prechlorate, pre-aligned	55.5	11	0.13	53.9	34	1.22

starting material. The barium is located in the 'as-formed' product as $BaFe_2O_4$. Some of the original iron fuel source has been consumed in the reaction. This has either combined with Fe_2O_3 and some oxygen to form Fe_3O_4, undergone a partial oxidation to form $Fe_{1-x}O$ or become incorporated in the $BaFe_2O_4$. The possibility that the iron has oxidised to Fe_2O_3 is also credible, although this cannot be quantified because Fe_2O_3 has been added as a moderator to the reaction. The oxidation process is summarised in Scheme 1. The zero field reaction was observed to propagate at 975 °C as detemined by optical pyrometry and 920 °C by thermal imaging camera. Electron microprobe analysis of the zero field samples showed the expected elemental ratios over large areas *ca.* 100×100 μm^2, Fig. 5a. Some fine grained regions could be distinguished on the micron scale which corresponded to formation of particles of $BaFe_2O_4$, $Fe_{1-x}O$, and Fe_3O_4 along with unreacted Fe, and Fe_2O_3. These regions showed no particular shape or orientation and appeared relatively randomly within the green mixture.

Reactions in an external magnetic field of 1.1 T

In the applied field reactions all of the starting material was drawn into the centre of the magnetic field to form a 3 cm long cylinder with an hour-glass configuration in cross section. The hour-glass shape was oriented relative to the field. In most experiments the long axis was vertical, although reactions with a horizontal orientation were also investigated (no differences were observed). The applied field synthesis wave was observed to be faster (5 mm s^{-1}) and hotter, 1150 °C by optical pyrometry and 1210 °C by thermal imaging camera than the zero field counterparts. The product from the reaction consisted of two portions, a fused shiny part that makes up 70% and a dull matt red–brown part. The shiny component had a fibrous appearance, with the shiny fibres parallel to one another and orientated in the direction of the magnetic field, Fig. 6. The shiny and matt components were manually separated, examined and sintered. The matt phase was shown to be multi-phasic with in order of abundance Fe_2O_3, $BaFe_2O_4$, Fe, $Fe_{1-x}O$ and Fe_3O_4 being detected. These phases closely matched that formed in the zero field reactions and corresponded to *ca.* 60% of the reactants being converted. The shiny component was also multiphasic, however in this case the phases in order of importance were Fe_3O_4, $BaFe_2O_4$, $Fe_{1-x}O$ and Fe_2O_3. No unreacted iron was detected and the conversion of the reactants was in excess of 90%. Intriguingly the shiny product showed a unique elemental microstructure by electron probe measurements. In these samples *ca.* 100×10 μm lozenges were found which contained barium to iron ratios of 1 : 12, as required for hexagonal barium ferrite. These lozenges were arranged almost parallel to their immediate neighbours (Fig. 4b). Between the lozenges were areas of partially reacted material that contained some $BaFe_2O_4$ and iron oxide. Some star shaped features were also observed. The matt portion of the applied field synthesis had the same overall large area 100×100 μm^2 elemental composition as the shiny fraction, however this sample showed a relatively uniform microstructure.

Table 4 Mössbauer parameters for sintered $BaFe_{12}O_{19}$ products. All the samples were modelled with sextets of areas in the ratio 12 : 6 : 4 : 2 for the 12k, ($4f_{IV}+2a$), $4f_{VI}$ and 2b sites respectively. The area of the Fe_2O_3 component (not shown minor phase) for the perchlorate products was unconstrained. Isomer shift ($\delta \pm 0.01$ mm s^{-1}), quadrupole shift ($\mathit{\Delta} \pm 0.02$ mm s^{-1}), linewidth ($\mathit{\Gamma} \pm 0.01$ mm s^{-1}) and hyperfine field ($B_{hf} \pm 1$ kG) are given for the various sites

Iron site within $BaFe_{12}O_{19}$[e]		ZF[a]	AF[b] nonmet	AF met	Pre-al[c] nonmet	Pre-al met[d]	BaFper[f] ZF	BaFper AF	BaFper pre-al	BaF ceram[g]
12k	δ	0.35	0.35	0.35	0.36	0.34	0.36	0.36	0.35	0.36
	$\mathit{\Delta}$	0.40	0.40	0.41	0.41	0.39	0.41	0.40	0.41	0.42
	$\mathit{\Gamma}$	0.28	0.28	0.29	0.28	0.35	0.27	0.27	0.27	0.28
	B_{hf}	413	411	413	413	410	411	413	412	413
$4f_{IV}+2a$	δ	0.27	0.27	0.28	0.28	0.26	0.27	0.26	0.27	0.28
	$\mathit{\Delta}$	0.20	0.20	0.20	0.21	0.21	0.22	0.20	0.21	0.19
	$\mathit{\Gamma}$	0.32	0.32	0.32	0.32	0.36	0.31	0.32	0.33	0.33
	B_{hf}	492	491	492	492	488	490	491	491	491
$4f_{VI}$	δ	0.38	0.38	0.38	0.38	0.38	0.39	0.39	0.39	0.39
	$\mathit{\Delta}$	0.14	0.15	0.15	0.15	0.12	0.15	0.15	0.21	0.13
	$\mathit{\Gamma}$	0.26	0.26	0.26	0.26	0.26	0.26	0.26	0.26	0.22
	B_{hf}	514	513	514	514	509	513	514	514	512
2b	δ	0.35	0.35	0.38	0.36	0.35	0.28	0.29	0.30	0.26
	$\mathit{\Delta}$	2.25	2.25	2.26	2.32	2.22	2.20	2.23	2.22	2.12
	$\mathit{\Gamma}$	0.47	0.42	0.47	0.58	0.48	0.53	0.60	0.65	0.51
	B_{hf}	400	399	398	399	398	400	398	398	397

[a] ZF = synthesis carried out with zero field. [b] AF = synthesis carried out under an applied field of 1.1 T. [c] Pre-al = synthesis carried out by aligning the green mixture with a 0.2 T field, the field is withdrawn prior to synthesis. [d] Met = metallic. [e] A minor *ca.* 2% component of $BaFe_2O_4$ was also detected. [f] BaFper = barium ferrite synthesised in the presence of sodium perchlorate. [g] Ceram = barium ferrite synthesised from a conventional ceramic method.

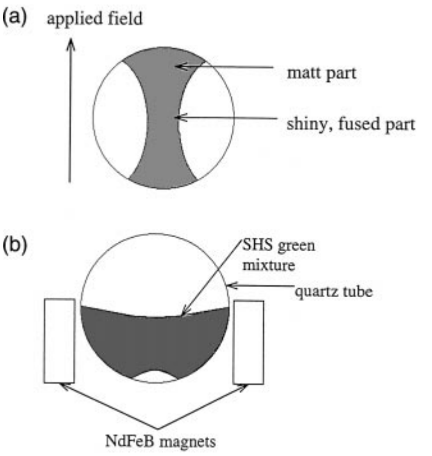

Fig. 1 (a) Alignment of the green mixture in the 1.1 T Halbach cylinder magnet, (b) alignment of the green mixture by the NdFeB magnets.

Reactions of pre-aligned powder

Reactions were performed in which the green mixture was magnetised inside a quartz tube by bringing two disks of NdFeB magnet up to the powder (Fig. 1b). This caused the green mixture to adopt a partial hour-glass cross sectional configuration. The NdFeB magnets were removed. Despite this the green mixture maintained the pseudo hour-glass cross sectional shape. The mixture was then ignited and a propagation wave passed through the solid at a temperature of 1080 °C as determined by thermal imaging camera, with a velocity 2 mm s^{-1}. The product from the reaction was composed of two parts, a matt red–brown powder which made up 70% and a shiny silver coloured globules which made up 30%. These silver globules had a partly fibrous surface structure. These parts were manually separated and analysed. Both samples were polyphasic. The matt component was comprised of unreacted iron, iron(III) oxide and some partly oxidised products Fe_3O_4, $BaFe_2O_4$ and $Fe_{1-x}O$. The shiny globular component contained little unreacted starting material and consisted of Fe_3O_4, $BaFe_2O_4$ and $Fe_{1-x}O$. Electron microprobe investigations of both the matt red–brown material and the shiny globular fraction revealed the same elemental compositions and a relatively homogeneous microstructure with no acicular particles.

Reactions using sodium perchlorate

Reactions were also studied in which an additional internal oxidising agent, sodium perchlorate, was added to the initial reaction mixture. Sodium perchlorate decomposes at the synthesis wave temperatures to form oxygen and sodium chloride. The amount of sodium perchlorate added to the initial mixture was adjusted such that it made up for all of the oxygen deficiency in the reaction [eqn. (2)]. Experiments were studied using sodium perchlorate in zero field, an applied field of 1.1 T and under pre-alignment conditions. The most notable feature of all the sodium perchlorate reactions irrespective of conditions was that no unreacted starting materials were detected in the products. The reactions were all at higher synthesis temperatures than the non-perchlorate analogues (Table 2). The products were black, fused, and with no evidence of a fibrous structure. In the applied field and pre-aligned samples a small 5–10% fraction of the sample had a shiny globular type appearance. No attempt was made to separate this product as had been the case for the non-perchlorate reactions. In all the sodium perchlorate reactions three principal phases were detected in the product. Listed in order of abundance these were Fe_3O_4, $Fe_{1-x}O$ and $BaFe_2O_4$ (Fig. 2c, 3b). An electron microprobe investigation of these materials indicated that the products were essentially homogeneous. Exceptions of *ca.* 10% for the applied field sample and *ca.* 5% for the pre-aligned sample were noted. In these cases evidence of acicular lozenge shaped particles similar to those seen in the shiny phase of the applied field non-perchlorate reactions were observed.

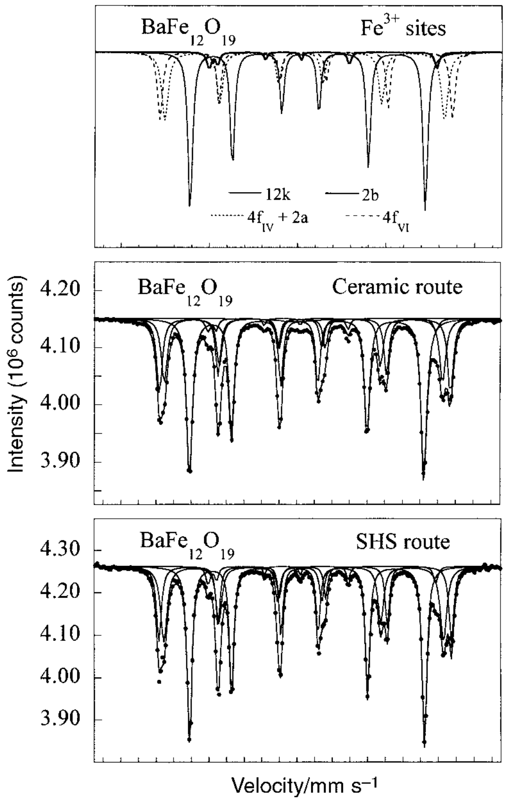

Fig. 2 Top: Mössbauer simulation of $BaFe_{12}O_{19}$ showing the sub-spectra corresponding to the 12k, $4f_{vi}$, $4f_{iv}+2a$ and 2b sublattice sites;[13] Middle: Mössbauer spectra of conventionally prepared $BaFe_{12}O_{19}$; Bottom: Mössbauer spectra of $BaFe_{12}O_{19}$ synthesised by SHS.

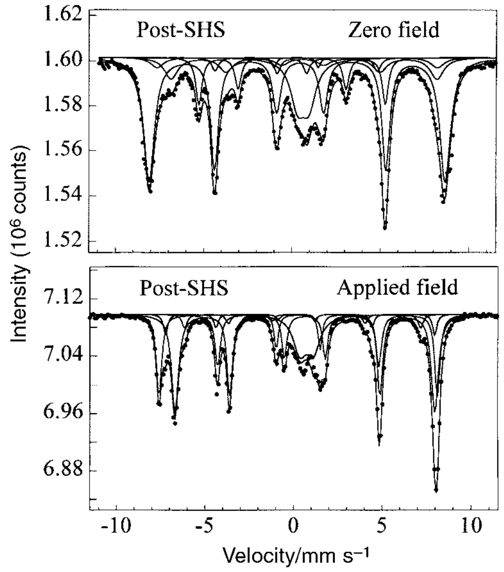

Fig. 3 Top: zero field post SHS product (the sextets from outer-most to inner-most are due to Fe_2O_3, Fe_3O_4, $BaFe_2O_4$ and Fe_3O_4 respectively; the inner doublet is due to FeO). Bottom: Mössbauer spectra of the applied field post SHS product (sodium perchlorate) (the sextets from outermost to innermost are due to Fe_3O_4, $BaFe_2O_4$ and Fe_3O_4 respectively; the inner doublet is due to FeO).

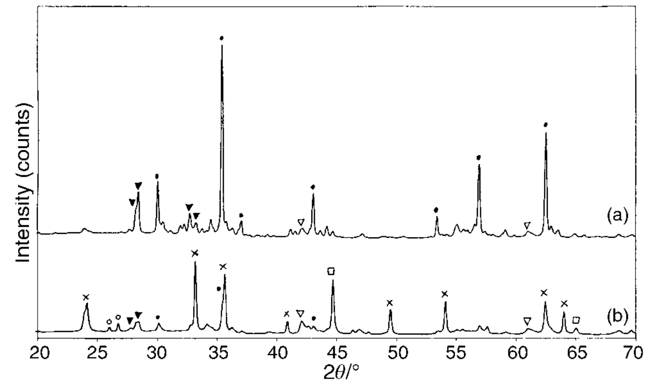

Fig. 4 (a) X-Ray powder diffraction pattern obtained from the applied field SHS reaction of BaO_2, Fe, Fe_2O_3 and $NaClO_4$; (b) X-ray powder diffraction pattern obtained from the zero field SHS reaction of BaO_2, Fe and Fe_2O_3. (● $=Fe_3O_4$, ▽ $=Fe_{1-x}O$, □ $=$ Fe, ▼ $=BaFe_2O_4$, × $=Fe_2O_3$, ○ $=BaO_2$.)

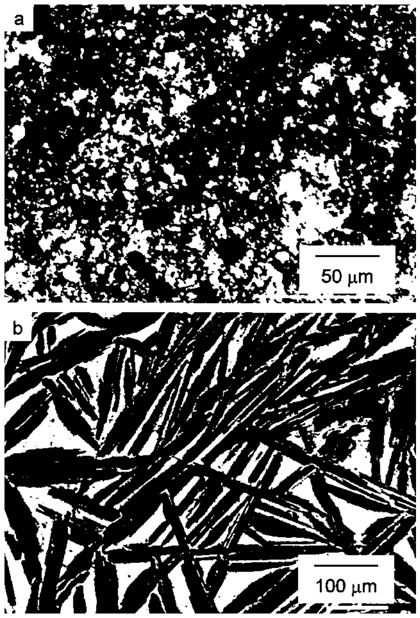

Fig. 5 Electron microprobe composition map of (a) the zero field SHS product and (b) the applied field SHS product (shiny part). The composition map is a grey scale of the abundance of iron, darker regions indicate iron rich areas.

Sintering of the products

Portions of all of the products from the various reactions described above were sintered at 1150 °C for 6 h. In all cases hexagonal barium ferrite, $BaFe_{12}O_{19}$ was formed. The barium ferrites were analysed by X-ray powder diffraction, scanning electron microscopy, energy dispersive analysis by X-rays, vibrating sample magnetometry and Mössbauer spectroscopy. The X-ray powder diffraction patterns for all samples indexed with a hexagonal cell with parameters that were identical or very similar to those reported for $BaFe_{12}O_{19}$, Fig. 6 (Table 1). Conventionally prepared $BaFe_{12}O_{19}$ has been indexed on a number of occasions with cell parameters; $a=5.889(1)$ Å, $c=23.190(7)$ Å;[12] $a=5.892(3)$ Å, $c=23.198(8)$ Å[18] and $a=5.8945(5)$ Å, $c=23.215(3)$ Å.[19] In the SHS prepared samples all of the a parameters fell between 5.885(2)–5.895(3) Å indicating identical values to conventionally prepared material within the 3σ criteria. The c parameters of the SHS prepared material showed a greater variation from 23.210(10)–23.260(12) Å. The difference between the SHS and conventionally prepared material may be significant, all of the SHS materials show larger c values and in a couple of cases the indexed error limits are above the 3σ criteria. It should be noted that in a few of the SHS samples a small amount of a second $BaFe_2O_4$ phase was also seen (*ca.* 2%). Scanning electron microscopy analysis showed the presence of hexagonal crystallites of micron dimensions, whilst spot energy dispersive analysis on all the samples gave the expected elemental ratios for $BaFe_{12}O_{19}$ over a number of spots. In the reactions that utilised sodium perchlorate, no sodium or chlorine could be detected in the sintered product by energy dispersive analysis, presumably because it was completely removed by washing the sample with water. Vibrating sample magnetometry showed significant differences in the magnetisation values between samples prepared under different conditions, this is discussed below. The sintered ferrites showed single phase $BaFe_{12}O_{19}$, by Mössbauer, Fig. 2. The spectra were fitted to the multiple site model of $BaFe_{12}O_{19}$ with subspectra corresponding to the 12k, $4f_{iv}+2a$, $4f_{vi}$ and 2b sublattice sites,[13] Table 4. No significant differences were observed by Mössbauer spectroscopy for the zero field or applied field synthesis. Mössbauer results of the sintered ferrites agree well with conventionally made materials.

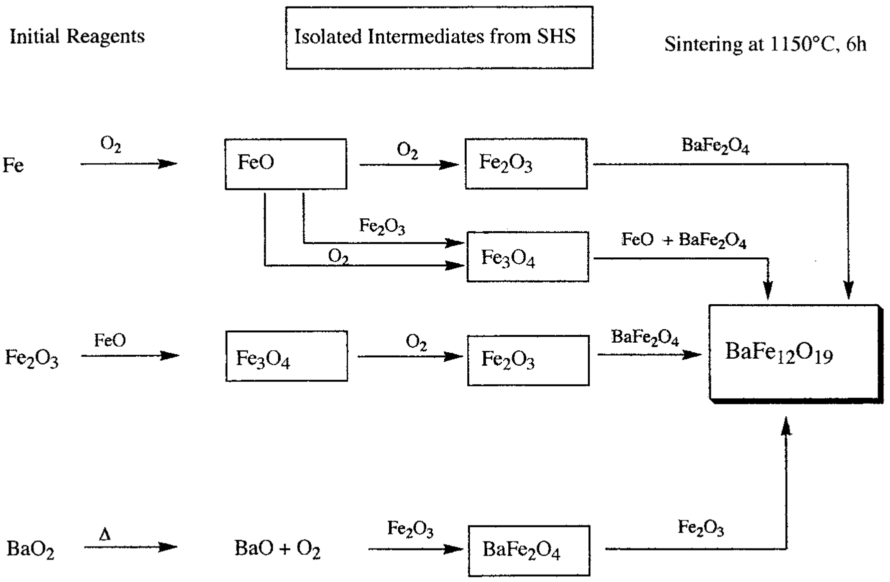

Scheme 1 Possible reaction pathways for the SHS reaction of BaO_2, Fe and Fe_2O_3.

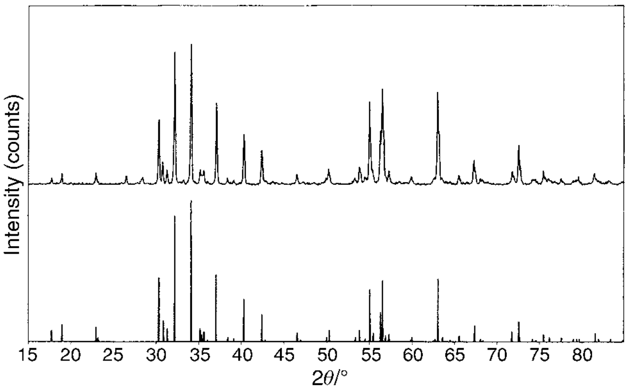

Fig. 6 Top trace; X-ray powder diffraction pattern of $BaFe_{12}O_{19}$ synthesised by SHS in zero field after sintering at 1150 °C for 6 h. Bottom trace; X-ray powder diffraction stick pattern for $BaFe_{12}O_{19}$.

Discussion

Completeness of the initial SHS reaction

A direct correlation was observed between the synthesis wave temperature and the completeness of the reaction. The zero field reactions had the lowest propagation wave temperature of 950 °C and the highest amount of unreacted starting material, whilst the sodium perchlorate reactions typically contained less than 10% unreacted material and had the highest synthesis wave temperature of 1250 °C. The principal reason that the sodium perchlorate reactions proceeded further is related to the oxygen released on sodium perchlorate decomposition. The reaction of BaO_2, Fe and Fe_2O_3 is essentially oxygen deficient and requires oxygen to enable the complete oxidation of the iron metal fuel source. In the zero field reactions this oxygen comes from the gaseous oxygen that is pumped into the reaction. However this oxygen flow is limited and is required to diffuse through the grains of the reactant powders. In the sodium perchlorate reactions, oxygen is released by the decomposition of the perchlorate. This oxygen is released throughout the powder rather than being limited to the diffusion controlled surface layers in the non-perchlorate reactions. The perchlorate also has a further function in the reaction; decomposition of sodium perchlorate generates heat which promotes the process and co-produced sodium chloride melts at the synthesis wave temperature and acts as a wetting agent to help the progression of the synthesis wave from one reactant layer to another.

The zero field SHS reactions were noted to be at lower temperatures than the applied field reactions. In the applied field synthesis the starting material is attracted into the centre of the magnetic field and adopts an hour-glass shape in cross section. It is possible that the starting components are separated in the magnetic field and this accounts for the higher synthesis wave temperatures. This was tested by experiments at the synchrotron laboratory at Daresbury on station 16.4. This allowed an analysis of the starting green mixture in the magnetic field. X-Ray diffraction patterns of the green mixture at different sample heights were recorded. The X-ray beam used in the experiments had a width of 0.1 mm. Thus it was relatively easy to see whether any of the green mixture had been preferentially pulled to the poles of the magnet, for example whether the magnetic iron component was dragged to the top and bottom of the magnet. Suprisingly the XRD patterns recorded at 6 different positions from within 2 mm of the magnet wall, through the centre of the sample to 4 mm from the top wall showed identical XRD patterns. Hence the green mixture maintains the same macroscale homogeneity in the magnetic field as it does in zero field. However on the microscopic scale it is likely that the iron powder is aligned with the field lines. One piece of evidence for this is that the shiny fibrous macrostructure was only seen in the applied field synthesis (Fig. 7). The shiny material is fibrous and aligned in the direction of the magnetic field. Further the electron microprobe of the shiny part shows evidence for acicular grains, perhaps corresponding to the pathway of the reaction front.

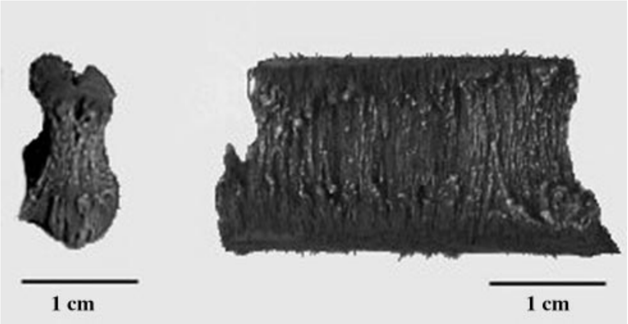

Fig. 7 Side and front elevations of the fused product formed in the applied field SHS reaction of BaO_2, Fe and Fe_2O_3.

The ease of SHS synthesis was directly related to the particle size of the initial iron powder. The fastest rate of propagation was observed for the smallest particle size. The very large particles of iron >500 μm failed to promote a propagation wave and a reaction could only be promoted by heating a bulk sample. The rate of reaction propagation is related to the ease of oxidation of the iron powder. This in turn is a consequence of the oxygen released in the reaction and the surface area of the iron powder. With large iron particle sizes the total surface area is relatively small and the reaction fails to propagate.

The sintered hexagonal ferrites have identical chemical compositions, lattice parameters and Mössbauer parameters irrespective of the exact reaction conditions, for example use of an applied external field or sodium perchlorate. However the magnetic properties of the materials are somewhat different. The samples synthesised in zero field, the applied-field matt portion and the pre-aligned matt portion when sintered had coercivities in the range 2.14–2.35 kOe. The shiny applied-field samples, the perchlorate samples and the pre-aligned metallic portions after sintering showed significantly lower coercivities, in the range 1.22–1.82 kOe. The coercivity of the samples after sintering seems to be related to the microstructure and the completeness of the reaction after the initial SHS stage. The coercivities compare to those measured for a commercial sample supplied by Sakai Chemical Industries of 2.66 kOe. The shiny components and the perchlorate samples are more fully reacted after SHS thus it is likely that grain growth during sintering is more favorable than in the less reacted parts. The larger grain growth during sintering would be expected to cause a reduction in coercivity.

Shiny *vs.* matt component

Shiny looking components were seen as part of the product in all reactions in an applied field of 1.1 T and in the premagnetised sample reactions. A different minor black/shiny component was also observed in reactions in which sodium perchlorate was used, even for the reactions in zero field. The fused shiny phase is a consequence of the reaction temperature; a synthesis wave over 1050 °C encourages formation of the shiny phase. The shiny component is grey in colour and partially reflective. In all systems it is essentially an electrical insulator. In some ways this component resembles a glaze formed in many ceramic syntheses. However the shiny component is uniform when broken into pieces and not restricted to a surface layer. The shiny particles formed in an applied magnetic field had a fibrous structure and were aligned in the direction of the magnetic field (Fig. 7). Sintering of either the shiny or matt component leads to black hexagonal barium ferrite.

The acicular microstructure

Acicular compositional microstructure (Fig. 5b) is only present in the shiny component of the applied-field SHS reaction. Notably in the pre-aligned SHS reactions no acicular particles were seen. This is unexpected as these two experiments are similar. The green mixture is the same, the shape of the reactants is similar (hour-glass in cross section), and the possible rearrangement of the particles within the green mixture is likely to be the same. A significant difference between these two reactions was that the magnetic field was removed from the pre-aligned reactions before SHS. Thus the occurrence of the acicular microstructure is a consequence only of having an applied magnetic field present during SHS. It is intriguing to speculate why the applied field has this effect. It is possible that the applied field can affect the propagation front of the reaction. Further work is planned at the Daresbury Laboratory to investigate these effects. It is possible that in the pre-aligned powder once the magnetic field has been withdrawn the powder still maintains the same macroscopic shape but on the microscopic level the components are somewhat randomised, unlike the case in which a field is applied during the reaction.

Conclusions

Self-propagating high temperature synthesis offers a fast, relatively straightforward two-step method for the synthesis of hexagonal-ferrites. The ferrites formed have equivalent properties to conventional ferrites including lattice and Mössbauer parameters, saturation magnetisation and remanent magnetisation. The use of an applied field during SHS affects the shape of the green mixture and the speed and temperature of the propagation wave. It also gives rise to a shiny-fibrous and a matt-coloured component. The shiny component shows an unusual microstructure consisting of lozenge shaped particles. The initial SHS reaction does not form single phased hexagonal ferrites. The reaction is promoted by the oxidation of iron metal. This oxidation reaction is limited by the availability of oxygen in the system. An internal oxidising agent, such as sodium perchlorate, increases the oxidation rate and progression of the reaction. A sintering phase is required to complete all of the SHS reactions, this is short compared to commercial processes, the as-formed SHS material being readily sinterable to single phase barium ferrite. Notably the ferrites formed from this two step procedure have significantly lower coercivity than conventional material. A lowering of the coercivity in hexagonal barium ferrite is accomplished by chemical doping, and is an important control factor for magnetic pigment and tape applications.

In a wider context an external magnetic field was shown in these studies to influence a series of chemical combustion reactions. In this system the prior organisation of the starting powder by the magnetic field forming an hour-glass shape, as well as an alignment of the magnetic particles along field lines were important factors. The appearance of the acicular electron microprobe elemental distribution was only prominent when an external field was present during the reaction. This indicates that the field has an effect on the combustion front during the reaction. Further studies are planned to explore the scope of external fields on other chemical reactions.

Acknowledgements

M.V.K. thanks the Royal Society and the Royal Society of Chemistry Journals Department for travel grants to the UK. The Mössbauer spectra were obtained *via* the University of London Intercollegiate Research Service. L.A. thanks the EPSRC for a studentship. FLIR systems International Ltd. are thanked for the loan of a thermal imaging camera. We are grateful to Simon Clark and Mark Roberts of the CLRC Daresbury Laboratory for their assistance on Stations 16.4 and 9.1 respectively and to Andrew Steer at UCL for help with the image plate XRD measurements.

References

1 A. G. Merzhanov, *Self-Propagating High temperature Synthesis: Twenty Years of Search and Finding* in *Combustion and Plasma Synthesis of High-Temperature Materials*, eds. Z. Munir and J. B. Holt, VCH, New York, 1990, p. 1.

2 A. G. Merzhanov, *Self Propagating High Temperature Synthesis and Powder Metallurgy: Unity of Goals and Competition of Principles* in *Advances in Powder Metallurgy and Particulate Materials*, Vol 9, 1992, Metal Powder Industries Federation, Princeton, NJ, p. 341.

3 B. Z. Shakhashiri, *Chemical demonstrations, a Handbook for Teachers of Chemistry*, University of Wisconsin Press, London, 1983, vol. 1., p. 85.

4 A. G. Merzhanov, *J. Mater. Process Technol.*, 1996, **56**, 222; A. G. Merzhanov, *Adv. Mater.*, 1992, **4**, 294; A. G. Merzhanov, *Int. J. Self-Propag. High Temp. Synth.*, 1995, **4**, 323.

5 A. G. Merzhanov *SHS Research Development Handbook*, ISMAN, Chernogolovka, p. 1.

6 J. B. Wiley and R. B. Kaner, *Science*, 1992, **255**, 1093; L. Rao and R. B. Kaner, *Inorg. Chem.*, 1994, **33**, 3210; E. G. Gillan and R. B. Kaner, *Inorg. Chem.*, 1994, **33**, 5693; A. L. Hector and I. P. Parkin, *Chem. Mater.*, 1995, **7**, 1728; I. P. Parkin, A. M. Nartowski, A. J. Craven, M. Mackenzie and I. Macloed, *J. Mater. Chem.*, 1999, **9**, 1275.

7 I. P. Parkin, *Chem. Soc. Rev.*, 1996, 199; E. G. Gillan and R. B. Kaner, *Chem. Mater.*, 1996, **8**, 333; A. L. Hector and I. P. Parkin, *Chem. Mater.*, 1995, **7**, 1728; I. P. Parkin, A. M. Nartowski, A. J. Craven, M. Mackenzie and I. Macloed, *J. Mater. Chem.*, 1999, **9**, 1275.

8 I. P. Parkin, *Chem. Ind.*, 1997, 725.

9 M. D. Aguas, G. C. Coombe and I. P. Parkin, *Polyhedron*, 1998, **17**, 49.

10 I. P. Parkin, A. V. Komarov and M. Odlyha, *J. Mater. Sci.*, 1996, **31**, 5033.

11 R. Pampuch, *Int. J. Self-Propag. High Temp. Synth.*, 1997, **6**, 187.

12 I. P. Parkin, G. E. Elwin, A. V. Komarov, Q. T. Bui, Q. A. Pankhurst, L. Fernandez Barquin and Y. G. Morozov, *J. Mater. Chem.*, 1998, **8**, 573; M. D. Aguas, L. Affleck, I. P. Parkin, M. V. Kuznetsov, A. Steer, Q. A. Pankhurst, L. Fernandez Barquin, M. A. Roberts, M. I. Boamfa and J. A. A. Perenboom, *J. Mater. Chem.*, 2000, **10**, 235.

13 I. P. Parkin, M. V. Kuznetsov and Q. A. Pankhurst, *J. Mater. Chem.*, 1999, **9**, 273; I. P. Parkin and Q. A. Pankhurst, *Mater. World*, 1998, 743.

14 I. P. Parkin, M. V. Kuznetsov and Q. A. Pankhurst, *J. Mater. Chem.*, 1999, **9**, 643.

15 M. V. Kuznetsov, I. P. Parkin and Q. A. Pankhurst, *J. Phys. D.*, 1999, **32**, 2590.

16 M. V. Kuznetsov, Q. A. Pankhurst and I. P. Parkin, *J. Mater. Chem.*, 1998, **8**, 2701.

17 L. Affleck, W. Cross, M. V. Kuznetsov, I. P. Parkin and Q. A. Pankhurst, *J. Mater. Chem.*, 1999, **9**, 2545; I. P. Parkin, M. V. Kuznetsov, L. Fernandez Barquin and Q. A. Pankhurst, *Int. J. Inorg. Mater.*, 1999, **1**, 311.

18 A. Townes, *Z. Kristallogr.*, 1967, **125**, 437; H. Shin and S. J. Kwon, *Powder Diffr.*, 1992, **7**, 212.

19 W. Ng-Wang, *Powder Diffr.*, 1988, **3**, 249.